VOLUME RENDERING OF POOL FIRE DATA

by

Holly Rushmeier, and Anthony Hamins
Building and Fire Research Laboratory
National Institute of Standards and Technology
Gaithersburg, MD 20899
and
Mun Young Choi
University of Illinois
Department of Mechanical Engineering
Chicago, IL

Reprinted from IEEE COMPUTER GRAPHICS AND APPLICATIONS, Vol. 15, No. 4, 62-66, July 1995.

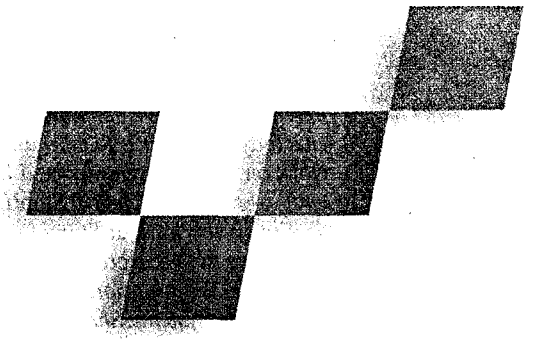

Volume Rendering of Pool Fire Data

Holly Rushmeier and Anthony Hamins
National Institute of Standards and Technology

Mun Young Choi
University of Illinois at Chicago

Ray casting, line integration, and other computer graphics techniques help visualize pool fire data and compute the radiative effects from these fires.

In a pool fire, an ignited puddle or pool of liquid fuel burns in the atmosphere. Understanding pool fires is important to devising methods to control the hazards resulting from spilled fuels. In this case study we consider techniques for visualizing the data measured in pool fires and for computing the radiative transfer from pool fires.

Combustion challenges the development of appropriate visualization techniques. Fires are turbulent, nonsteady, and multi-wavelength in emission. Moreover, fire data belongs to a class of visualization problems for which it is important to consider the radiative simulation used to generate visualizations.

We see objects as a result of the visible light they emit, transmit, or reflect. All rendering methods in some way simulate the radiative transfer of light.[1] When visualizing abstract representations of objects—such as molecular models—simple, heuristic rendering methods suffice. This is particularly true in volume visualization, in which a complete physical simulation of light propagation can be extremely computationally demanding.[2] However, in some volumetric problems radiative transfer is a critical part of the phenomena being visualized. For these problems, using radiometrically accurate techniques to generate images of the data can provide useful insights.

In the case of fire data, radiative transfer plays two important roles. First, data is obtained from fires by detecting radiation. Probes inserted in the fire measure radiative transfer over short distances. Qualitative information about the fire comes from simply observing the luminosity of the flame. Second, a major quantity of interest is the radiation from the fire that reaches surrounding surfaces. For example, the flame can ignite adjacent pools of fuel by radiative heat transfer. Using techniques to accurately image fire data, we can also make efficient calculations about the fire's impact on its surroundings.

We used basic tools to image fire data and to compute irradiation—efficient ray casting and radiometrically accurate line integrations. As we show here, visualization techniques help answer a number of questions about pool fires.

Problem description

In the experiment considered here, we took data for a 10-cm-diameter heptane pool fire. We used a pair of opposed, water-cooled, nitrogen-purged, intrusive probes separated by 12 mm, which defined the optical path. Another publication[3] describes the three-line optical sensing device, which uses amplified silicon diode detectors and narrowband filters.

Figure 1 diagrams the fire and typical measurement locations. A circular burner geometry ensures axial symmetry. Because the time-averaged flame is symmetric, we took data only for varying radii r from the center of the pool and for height z above the pool. Local instantaneous temperature, soot-volume fraction (volume of soot per unit volume of gas), and CO_2 concentrations were determined from radiation measurement in three wavelength regions (900 nm, 1,000 nm, and 4,350 nm). We used these data to estimate the concentrations of H_2O and CO.

Typical data locations appear in 2D plots in Figure 2. Details of the experimental procedure are given elsewhere.[3] We obtained these data to examine various features of radiative transfer from the fire.

In this case study we consider how visualization and graphical techniques used with this data can answer the following questions:

Question 1: How well do the measurements represent the actual data? The 2D plots shown in Figure 2 are difficult to relate to one another and to the luminous flame observed in the laboratory.

Question 2: What is the importance of radiation from the gases relative to radiation from the soot? Usually in the past only soot has been considered.

Question 3: What is the radiative feedback to the fuel surface? How much heat does the flame contribute to the pool surface for vaporization?

0272-17-16/95/$4.00 © 1995 IEEE

Question 4: What is the irradiation at points in the space around the fire? At what distance from the fire would other materials be affected? For example, serious injury and blistering of human skin begin to occur after 20 seconds exposure to radiative fluxes equal to 4,000 W/m^2.

Ray casting and line integration

The basic tool for imaging and computing radiative transfer is ray casting. Figure 3 diagrams casting a ray through the volume of data. Because we collected data only at varying r and z, the volume of data is a stack of cylindrical rings. Rays are simply followed from the observer (or, in the case of irradiation calculations, from the collector position) through the cylinder. For each ring encountered, the next pierce point is found. If the wall of the ring is pierced, the r index is incremented (or decremented) to find the next ring encountered, else the z index is incremented or decremented.

Having found the complete traversal of the ray, we construct a list of the ring segments through which the ray passes. For each segment distance, we collect temperature, soot-volume fraction, and gas partial pressure. These data go to the radiation-calculating routine RadCal,[4] which performs the line integration yielding intensity $i(l)$ (energy per unit of projected area, time, and solid angle, referred to as radiance in the lighting and graphics literature) at the end of the ray path l. RadCal accurately calculates the radiation, taking into account the detailed spectral properties of CO_2, H_2O, CH_4, CO, N_2, O_2, and soot. Grosshandler[4] presented RadCal as an independent Fortran program (he included code in the publication). However, you can readily adapt it to a callable subroutine. RadCal evaluates the following equations to obtain $i(l)$:

$$i(l) = \int_{\lambda_1}^{\lambda_2} i_\lambda(l)\,d\lambda$$

$$i_\lambda(l) = i_{\lambda,w}\, e^{-\kappa_\lambda(l)} + \int_0^{\kappa_\lambda(l)} i_{b,\lambda}(l^*)\exp\left[(\kappa_\lambda(l)-\kappa_\lambda(l^*))\right]d\kappa;$$

$$\kappa_\lambda \equiv \int_0^l a_\lambda(l^*)\,dl^* \qquad (1)$$

Here, λ is wavelength, and λ_1 and λ_2 are the limits of the wavelength band of interest for the calculation. For irradiation calculations, the band can be the entire infrared spectrum. Or, we could consider narrow bands for the purpose of examining radiation in the visible, or other bands of interest. The optical thickness of the medi-

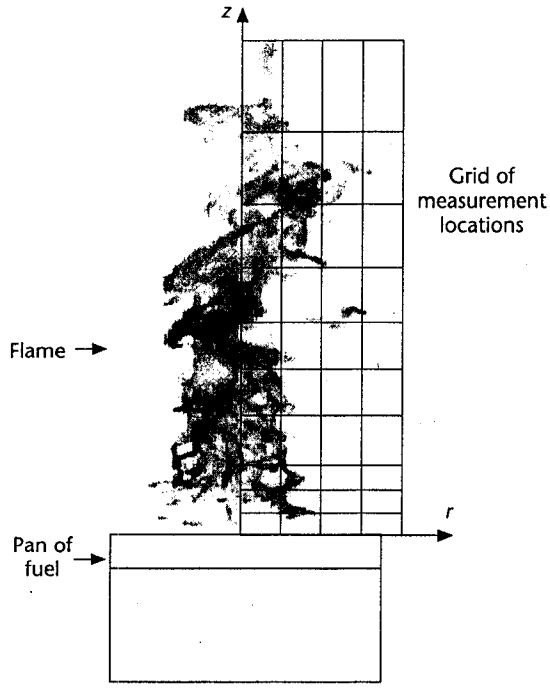

1 Typical locations for taking pool fire data.

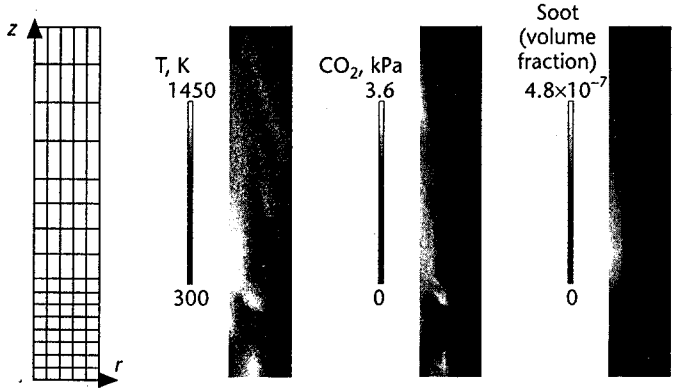

2 Typical temperature, CO_2 partial pressure, and soot-volume-fraction data for a pool fire. The data are shown in 2D gray-scaled plots.

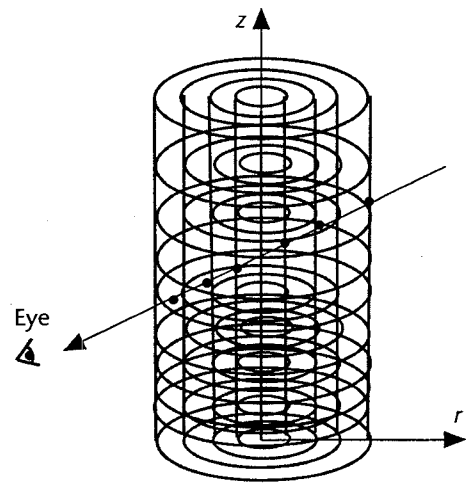

3 Using the measured data, the fire is numerically modeled as a stack of cylindrical rings, with uniform properties in each ring. To generate images or calculate incident irradiation, rays are cast through the numerical model, and the points where the rays pierce each cylindrical ring are found.

4 Images of the visible flame grabbed from videotape: (left) individual frame, (middle) individual frame grabbed one second later, and (right) average of the 30 frames beginning with the image at the left and ending with the image in the middle.

um, κ_λ, is by definition a function of the absorption coefficient a_λ (fraction of intensity absorbed per unit length)along the path. The spectral intensity at the beginning of the ray path is $i_{\lambda,w}$. For the pool fire problem, we take this to be the black-body intensity (that is, the spectral distribution given by the Planck distribution function) at normal room temperature (about 300 K). The black-body intensity along the path is $i_{b,\lambda}(l^*)$.

RadCal considers only absorption and emission along the path—not scattering, since the effect is negligible for the problem of radiation in combustion products. RadCal assumes local thermodynamic equilibrium (LTE), which is an accurate assumption for the radiative transfer of interest in thermal problems. That is, all the radiation is assumed to result from thermal agitation, which is directly indicated by the medium's temperature. Note that non-LTE radiation—that is, the luminescence from excitation other than thermal agitation—causes a significant amount of visible radiation in some types of flames, particularly flames that appear blue. However, visible radiation in most fires, such as the heptane pool fire considered in our example, is dominated by LTE radiation from soot particles.

Generating images

Forming images can help us answer the first two questions raised earlier. Generating images of the fire using a synthetic camera defined with various spectral sensitivities lets us qualitatively answer questions such as how well the data describe the fire and the relative importance of gas versus soot radiation.

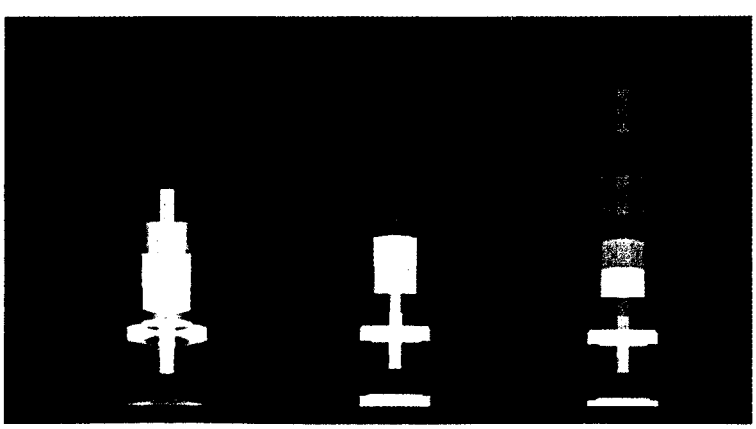

5 Synthetic images from measured temperatures and concentrations: (left) image generated using data averaged from 2,000 time samples, (middle) image generated using data averaged from 30 time samples, and (right) image generated by averaging images of 30 time samples.

One way to evaluate the measurements is to view the measured data in the same manner as we physically observe the fire. We image the luminous flame by computing radiances in the visible band and performing appropriate perceptual transformations to produce a true color image. For the most accuracy, we would use RadCal to calculate spectral intensities in the range of 400 nm to 700 nm, then convolve these intensities with the CIE $X(\lambda)$, $Y(\lambda)$ and $Z(\lambda)$, functions for the human visual system, and convert from *XYZ* coordinates to *RGB* by using measured monitor characteristics.[5] Because the radiated spectrum from the soot is relatively smooth, to generate images rapidly we sampled the spectrum at the peaks of the *X*, *Y*, and *Z* curves only, estimating the ratios *X*:*Y*:*Z*. The sample spectral intensities are in units of watts per meter squared steradian. These intensities must be scaled to CRT display values in the range 0 to 255. Again, to generate images rapidly, we displayed the results by simply scaling the average luminance value to a value of 128 in the final image.

For the purposes of comparison, Figure 4 shows video images of the actual fire. We used an uncalibrated video camera, and the flame colors in the video look quite desaturated compared to the colors observed directly in the laboratory. Figure 4 left and middle show individual frames grabbed one second apart. The individual frames show the complex, turbulent shape of the fire and indicate the short time frame in which the variation in shape occurs. Figure 4 right is the average of 30 images grabbed from videotape of the actual pool fire. It shows the nearly axisymmetric structure of the time-averaged flame.

Figure 5 shows synthetic images generated from measured data. We took 2,000 measurements at each spatial location in succession (2,000 at r_1, z_1, then 2,000 at r_2, z_2, and so on). We generated Figure 5 left using the average of all 2,000 values at each location. As expected, the synthetic image shows that the spacing of the measurements doesn't represent the geometric detail of the flame. However, the measurements are adequate to capture the necking in of the flame near the fuel surface and the broadening further above the surface. Additional spatial measurements are needed to completely characterize the time-averaged structure.

Figure 5 middle and right illustrate the difference between an image from time-averaged measurements and time-averaged images from a time series of measurements. We generated the image in Figure 5 middle using the average of 30 measurements at each location. The image in Figure 5 right was generated by averaging 30 images, each generated using just one of the

30 measurements at each location. That is, even though the data weren't taken simultaneously, we constructed artificial instantaneous data sets by using the first data measured for each location, the second data, and so forth. Because intensity values must be clipped for each image, the image in Figure 5 right is desaturated similar to the averaged video image in Figure 4 right.

Comparing Figure 5 middle and right shows a substantial difference between the image from averaged data and the averaged image. This is significant because the images result from making a physically accurate estimate of the radiation from the data set. The images indicate that the magnitude and spatial distribution of the radiation from the fire using instantaneous data differs significantly from the averaged data.

We could make more accurate estimates of radiative transfer effects if we could make measurements at several locations simultaneously. Since such simultaneous measurements are substantially more expensive to obtain, we must be able to evaluate their usefulness.

Note the synthetic images in Figure 5 show no numerical legend. We did this because they are visual simulations, not pseudocolored displays.

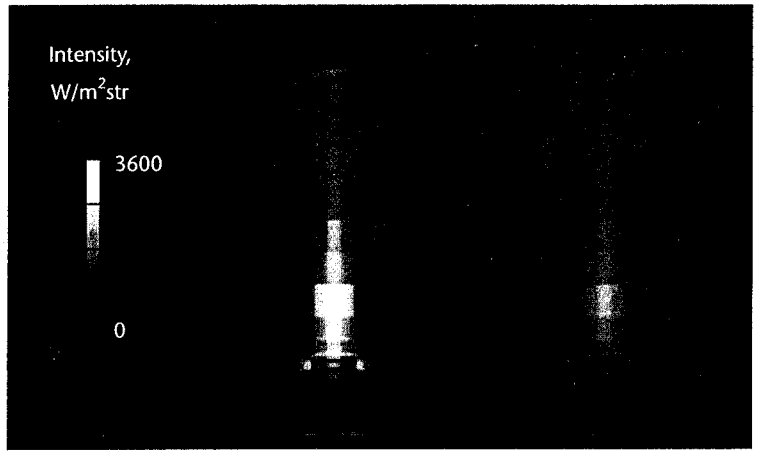

6 Infrared images of radiation from soot and gas (left) versus soot alone (right).

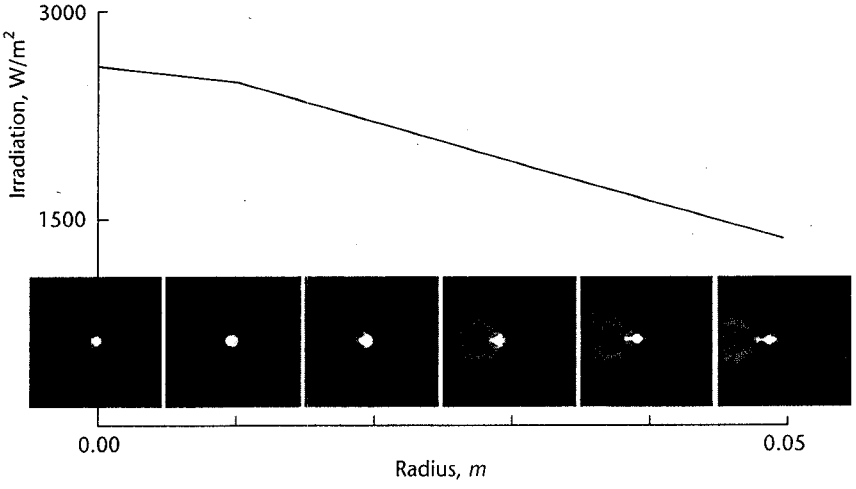

7 The graph shows the irradiation of the pool surface by the hot combustion products as a function of radial position. The small images each show a wide-angle view from the pool surface, looking upward at the combustion products from the various radial positions.

Radiation from the fire in the visible range comes primarily from the soot. To gain insight into the relative importance of soot versus gas radiation, we must image the fire using a synthetic camera that integrates wavelengths throughout the infrared range. Figure 6 shows the resulting image when RadCal gets temperatures, soot-volume fraction, and gas partial-pressure data (on the left), versus the image that results when only temperatures and soot-volume-fraction data are used. A comparison of the figures shows that the gases are responsible for a significant amount of radiation. A numerical legend appears on these images, since the gray shades are assigned based on the total infrared intensity at each pixel, not on perceptual principles.

Computing and visualizing irradiation

The same ray-casting and line-integration techniques used to generate images can compute irradiance on surfaces around the fire. For example, the radiative feedback per unit area, $\dot{q}''(r)$ to a point on the pool surface at radius r, is given by

$$\dot{q}''(r) = \int_0^{2\pi} \int_0^{\frac{\pi}{2}} i(\theta,\phi)\cos(\theta)d\theta\, d\phi \qquad (2)$$

The angles θ and ϕ are respectively the polar and azimuthal angles of a coordinate system based on the pool surface. The intensity $i(\theta,\phi)$ is the incident intensity from direction (θ,ϕ). We find $i(\theta,\phi)$ by casting a ray in the direction (θ,ϕ) and computing $i(l)$ for that direction, as in Equation 1. We can evaluate the integral using a Monte Carlo method, summing up the results of casting rays in a large number of randomly chosen directions. Figure 7 shows typical results at $z = 0$ (the pool surface) and values of r from 0 (the center of the pool) to 0.05m (the edge of the pool) using the fire data given in Figure 2. Note, we show these results only as examples of the calculations; details of numerical results for total radiative feedback to the pool fire appear elsewhere.[3]

The rays cast to evaluate $i(\theta,\phi)$ in Equation 2 are the same as those cast to generate fish-eye views from a location on the pool surface looking up into the fire. Figure 7 also shows small, wide-angle (136-degree field of view) images for each of the points for which we calculated $\dot{q}''(r)$. These images provide several pieces of information.

First, the images serve as a valuable debugging tool for checking that the radiation calculations are being performed correctly. It is straightforward to check numerical results for a small number of rays, but not for the large quantity of rays needed to compute irradiation. The continuity of the images indicates that no special cases exist in which the ray casting fails and produces incorrect results.

Second, the images also illustrate why a large num-

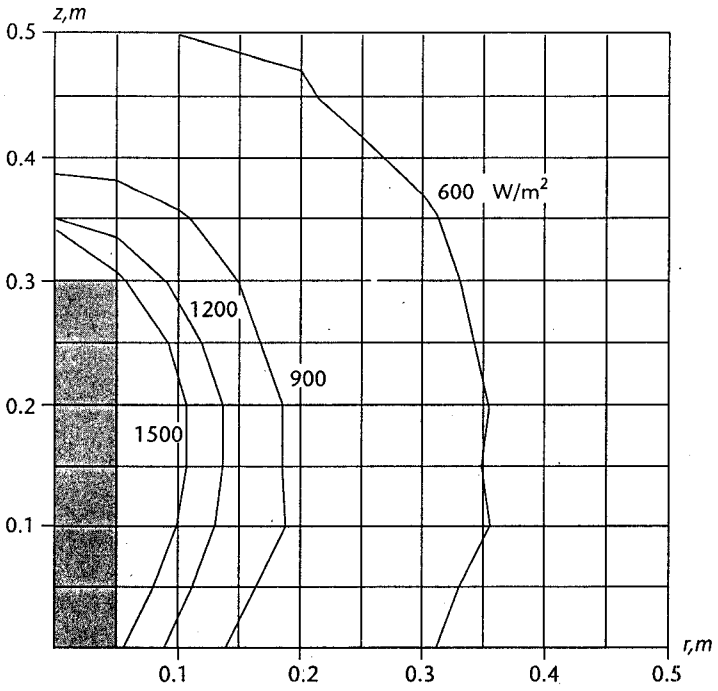

8 Two-dimensional plot of contours of constant irradiation for points around the pool fire.

ber of rays are needed to compute an accurate estimate of irradiation. Much of the radiation comes from a small hot spot that only a small fraction of random rays hit. This observation suggests that reformulating the irradiation calculation problem in the computer graphics form described by Kajiya,[1] with the small hot volumes categorized as infrared "light sources" and sampled separately, would produce a much more efficient algorithm for computing irradiation.

Finally, the small wide-angle images yield physical insight. There are two possible explanations for the rate of falloff of irradiation with radius. One possibility is that as r increases, the view of the fire is obscured by cold intervening media. The other possibility is simply the reduced solid angle subtended by the hot gases as r increases. The small images indicate that the falloff results primarily from the solid angle effect.

The incident flux $\dot{q}''$ at other surfaces around the fire also interests us, to study the potential for ignition of other materials. The incident flux is a function of position in the volume around the fire and orientation relative to the fire. To estimate the flux in the space around the fire, we evaluated Equation 2 for a grid of points in that space, with a surface normal vector oriented towards the center of the fire to estimate the maximum flux.

Because the fire data is rotationally symmetric, we can diagram the results in two dimensions as shown in Figure 8. However, this does not give a casual observer a good sense of the data's meaning—it doesn't communicate that the irradiation spreads through space and that it applies to surfaces oriented towards the fire.

Figure 9 shows a volumetric rendition of the irradiation data. We colored a collection of spheres according to the maximum incident flux at that location. A simple lighting heuristic highlights the sphere in the direction of the fire, to emphasize the role of orientation in the flux calculation. We might obtain an even more meaningful presentation by placing the fire in a model of a room and rendering the objects in the room with the fire as a volumetric infrared light source.

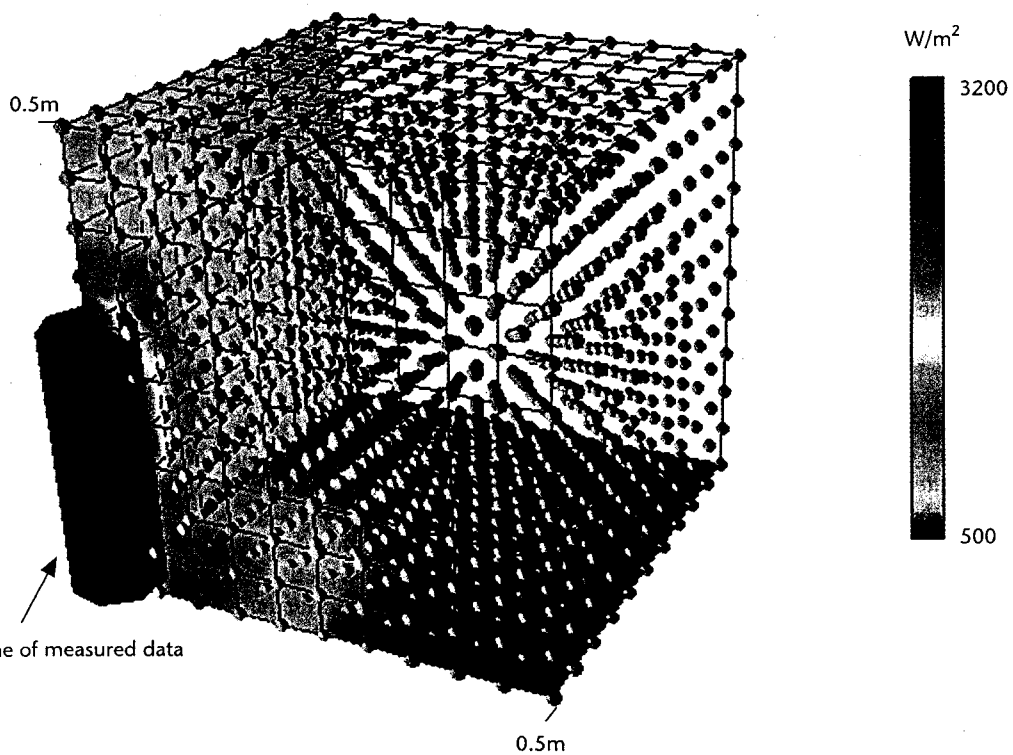

9 Three-dimensional representation of irradiation in the volume of space surrounding the pool fire.

Answers

We have shown how to use techniques from computer graphics to gain insight into data from pool fires. Specifically, we have answered the four questions posed in the "Problem description" section:

Question 1: How well do the measurements represent the actual data?

Answer: Comparing the video and synthetic images in Figures 4 and 5 indicates that we need additional spatial data and simultaneous measurements to characterize the fire if we want to examine radiative transfer effects.

Question 2: What is the importance of gas versus soot radiation?

Answer: Comparing the synthetic infrared images in Figure 6 shows that we cannot ignore the effect of gas radiation relative to soot radiation.

Question 3: What is the radiative feedback to the fuel surface?

Answer: The same ray-casting technique used to generate synthetic images serves to calculate radiative feedback. We can use wide-angle synthetic images from the pool surface to check the calculations and gain physical insight into the spatial distribution of the radiative flux.

Question 4: What is the irradiation at points in space around the fire?

Answer: Computer graphics techniques help show how the irradiation in the environment varies with both location and orientation.

Future work

We obtained the data in the examples given here using an immersive probe. Such a probe has the disadvantage that the entire temperature and emission distribution cannot be obtained simultaneously. An alternative approach for obtaining fire data involves imaging and applying techniques from tomography. A potential future role for synthetic images of fire data may be in the design of such imaging systems. Synthetic camera simulations could be used in determining the system geometry and in developing efficient algorithms for extracting data about fire structure from the images obtained.

Outside the laboratory, the geometric scale of many fires, such as burning oil spills, prevents the detailed measurement of the fire structure. Photographic images of the fires are an important method of data collection. Physically accurate visible and infrared images of numerical results from mathematical models used to predict large-scale fire structure could prove to be valuable validation tools.

The usefulness of the visualization techniques described here comes from recognizing the relationship between the physical radiative transfer from fires and the model of radiative transfer used to generate synthetic images for visualization. In other problem domains that apply visualization, it might be possible to develop more effective techniques by relating the radiative transfer used to acquire the data and the model of radiative transfer used to visualize the data. ■

References

1. J.T. Kajiya, "The Rendering Equation," *Computer Graphics* (Proc. Siggraph 86), Vol. 20, No. 4, Aug. 1986, pp. 143-150.
2. H.E. Rushmeier and K.E. Torrance, "The Zonal Method for Calculating Light Intensities in the Presence of a Participating Medium," *Computer Graphics* (Proc. Siggraph 87), Vol. 21, No. 4, July 1987, pp. 293-302.
3. M.Y. Choi et al., "Simultaneous Optical Measurement of Soot Volume Fraction, Temperature, and CO_2 in Heptane Pool Fire," *Proc. 25th (Int'l) Symp. on Combustion*, Aug. 1994, The Combustion Institute, Pittsburgh, pp. 1471-1480.
4. W.L. Grosshandler, "RadCal: A Narrow-Band Model for Radiation Calculations in a Combustion Environment," NIST Technical Note 1402, National Institute of Standards and Technology, Apr. 1993.
5. R. Hall, *Illumination and Color in Computer Generated Imagery*, Springer-Verlag, New York, 1989.

Holly Rushmeier *is on the staff of the Computing and Applied Mathematics Laboratory at the National Institute of Standards and Technology. Her research interests include scientific visualization, realistic image synthesis, and radiative heat transfer. Rushmeier received BS (1977), MS (1986), and PhD (1988) degrees in mechanical engineering from Cornell University.*

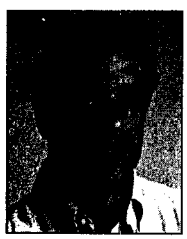

Anthony Hamins *has been with the Building and Fire Research Laboratory at the National Institute of Standards and Technology since 1989, where he is investigating the stability of flames and developing models of the heat and mass transfer processes that occur in fires. He completed his PhD in engineering physics at the University of California at San Diego in 1985.*

Mun Young Choi *is an assistant professor in the Department of Mechanical Engineering at the University of Illinois at Chicago. His research interests include characterization of laminar and turbulent diffuse flames by using optical and intrusive techniques. He received his bachelor's degree from the University of Illinois at Urbana-Champaign and his MA and PhD degrees from Princeton University.*

Readers may contact Rushmeier at Rm. B-146, Bldg. 225, National Institute of Standards and Technology, Gaithersburg, MD 20899, e-mail holly@cam.nist.gov.